CHINESE JOURNAL OF PHYSICS VOL. 52, NO. 2 April 2014

A Study of the Dependence of Electrohydrodynamic Jetting on the Process Parameters and Liquid Physical Properties

Kyung-Hyun Choi,[1,*] Kamran Ali,[1] and Khalid Rahman[2]

[1]*Department of Mechatronics Engineering, Jeju National University, Jeju 690-756, Korea*

[2]*Department of Mechanical Engineering, Ghulam Ishaq Khan Institute of Engineering Sciences and Technology, Swabi, Pakistan*

(Received July 13, 2012; Revised July 31, 2013)

The role of the applied voltage and liquid physical properties in the stable cone jet formation has been investigated in this paper. A higher pulse voltage of large duty cycles superimposed on a high bias voltage produced a stable cone jet under constant applied pressure. The critical voltage required for the formation of the stable cone jet decreased with an increase in the applied pressure for solutions having different conductivities. As compared to low viscous and high conductive solutions, high viscosity liquids with low conductivity were unable to form a stable cone jet easily at higher frequencies and low pulse time. The experimental results indicate that there is a strong relationship among these parameters, and a precise control of these parameters is required to achieve high quality electrohydrodynamic (EHD) jetting. Also five dimensionless parameters have been derived using the Buckingham Π theorem, and their effect on EHD jetting has been analyzed thoroughly.

DOI: 10.6122/CJP.52.799 PACS numbers: 47.65.-d, 47.61.-k

I. INTRODUCTION

Electrohydrodynamic (EHD) jetting is one of the novel technologies for depositing various kinds of functional materials for the fabrication of electronic devices, and it also has a great importance in the field of bio-applications [1, 2]. This technology has a unique reputation in the electronic industry because of its environmentally friendly nature, low fabrication cost, highly accurate targeting, and no need of a physical mask [3]. Also its non-contact printing nature eliminates the threat of the damage of fragile substrates while depositing onto them the functional material.

In electrohydrodynamic jetting, electrostatic forces are applied on the meniscus of a liquid, in order to release it from the nozzle opening by overcoming the surface tension forces, thereby pulling it towards the ground substrate. This special feature distinguishes this technology from other conventional printing techniques and gives it the ability of producing very high resolution patterns using nozzles of very small diameters [4]. Moreover this technique can be used to produce prints of highly viscous inks [5, 6]. Various kinds of materials can be deposited using electrohydrodynamic jetting [7–20].

*Electronic address: amm@jejunu.ac.kr

Electrohydrodynamic jet deposition can be divided into two modes: continuous mode [17, 21] and drop-on-demand mode [20]. In continuous mode, DC voltage is used to achieve continuous printing, this is most suitable for the direct writing approach of colloidal solutions. The speed and high velocity of the jet enables it to travel larger distances to the substrate. In continuous mode the scattering masses are significantly less for submicron resolution printing, and also the continuous flow of the ink through the nozzle minimizes the risk of its clogging during the process. Continuous mode only forms continuous lines, and therefore use of the continuous mode eliminates the requirement of overlapping of successive ink droplets to produce a continuous line [21]. Both modes are capable of producing high resolution patterns, but the control and stabilization of the high speed jet in the continuous mode is very difficult and can lead to unreliable printing [22]. In the case of drop-on-demand mode a pulse voltage is applied to the capillary for liquid charging instead of a continuous DC voltage, which causes the meniscus to deform into a cone and forming a droplet rather than a continuous jet, thus providing a greater control over the size and interval of the drop ejection [23]. When the drop is ejected, the surface tension forces dominate and the charge around the surface of the nozzle tip is decreased, due to which the meniscus is pulled back, and when the next voltage pulse is applied then another drop is produced [24].

The phenomenon of electrohydrodynamic jetting is greatly influenced by the nature and properties of the conducting liquids. Some of these properties include the conductivity, viscosity, and surface tension of the liquid [5, 25]. The liquid conductivity affects both the shape of the liquid cone and the jet stability by controlling the amount of electric charge on the liquid surface [26]. Viscosity plays a vital role in stabilization of the jet [6]. It enhances the jet stability through its effect on conductivity. In a viscous medium the ionic mobility is decreased, due to which both the conductivity and the radial electric field is decreased. Therefore, viscosity alteration is chosen as the main control parameter for jet stabilization. The surface tension of the liquid also plays an important role in the electrohydrodynamic jetting phenomena. When the surface tension near the conical apex is overcome by electrical forces, then the cone-jet transition takes place. Thus liquids having higher surface tension require higher electrical forces for jet formation [21].

This paper presents the relationships and the effects of the various properties of the conducting liquid on the jet stability, and also discusses the effect of the applied electric field on the drop formation. Hayati *et al.* [27] reported the influence of various parameters, such as the conductivity and electric field, but their work is related to electrostatic atomization, commonly known as electrospraying [13, 14]. The work presented in this paper is completely related to the electrohydrodynamic jetting phenomena. The experiments are performed using ethanol and four more solutions with different values of viscosity, conductivity, and surface tension. Different sets of experiments are performed by varying various process parameters, i.e., voltage, pulse time, pressure, and frequency. Both pulse and DC Voltage are used to study the different process parameters.

II. EXPERIMENTAL DETAILS

II-1. Solution preparation

To study the effects of liquid properties on the electrohydrodynamic jetting phenomena, four solutions were prepared. Ethanol was also selected for the experimentation as a reference material. Mixtures of ethanol and glycerin were used in the preparation of the solutions. Solution A has the composition of 75% ethanol and 25% glycerin. Solution B has 55% of ethanol and 45% of glycerin. The composition of solution C consists of 35% ethanol and 65% glycerin. The composition of Solution D consists of 25% ethanol and 75% glycerin. All the solutions have different values of viscosity, conductivity, surface tension, and dielectric constant which are summarized in Table I.

TABLE I: Physical properties of the solutions.

Sample name	Viscosity (mPa.s)	Conductivity (μS/cm)	Dielectric constant	Surface tension (mN/m)	Density ($\frac{kg}{m^3}$)	Hydrodynamic relaxation time (μ.sec)	Charge relaxation time (μ.sec)
Ethanol	1.6	0.3	25	22	780	8	7.37
Solution A	5.33	0.45	29	32.7	900	17.92	5.70
Solution B	34	0.12	33.1	41	996	91.21	24.4
Solution C	105	0.08	35.5	53.75	1218	214.88	39.2
Solution D	215	0.04	36.37	53.25	1140	444.13	80.4

II-2. Experimental Setup

The schematic of the experimental setup is shown in Fig. 1. A metallic capillary having an internal diameter of 110 μm (World Precision Instruments) was connected with an ink reservoir. The reservoir was mounted on a Z-axis stage to adjust the gap between the nozzle and substrate. The reservoir was then connected to the pressure regulator in order to supply the solution to the nozzle with a constant flow rate. The voltage was supplied by a high voltage power amplifier (Trek 610E) and controlled by a multifunctional signal synthesizer (HP 33120A). To control the substrate speed during the process, the ground plate was mounted on an X-Y motorized stage (SURUGA SEIKI DS102). The process was monitored with a high speed camera (Motion Pro X3), which was connected to the PC controller.

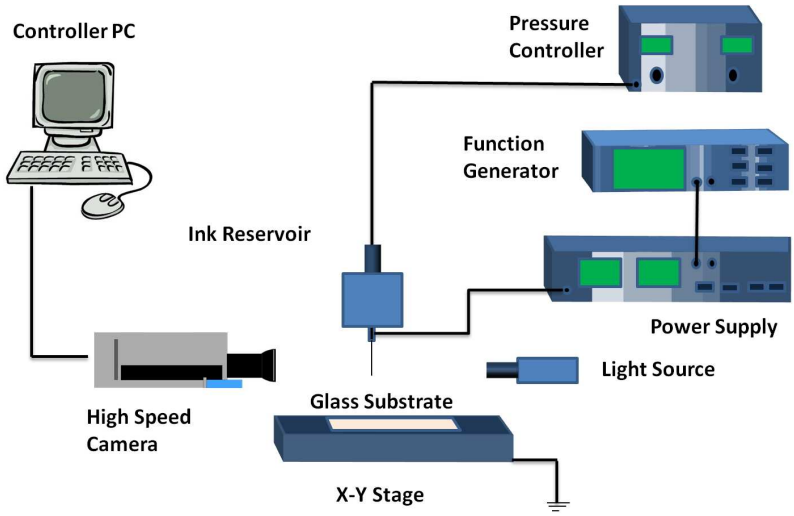

FIG. 1: Schematic diagram of the experimental setup used for electrohydrodynamic jetting.

III. RESULTS AND DISCUSSION

III-1. Effect of the applied voltage

III-1-1. Effect of the applied voltage on the pendant drop and on the cone shape

Fig. 2 shows the deformation of the pendant drop of solution B as a result of increasing the applied voltage of (2.74 kV – 3.5 kV). Under the applied pressure of 0.7 kPa the solution was supplied to the micro-capillary tip. The concentration of the charges on the droplet increases with an increase in the applied voltage, resulting in an increased electric force. The electric forces, together with the gravitational forces, act on the droplet and result in a decrease of the critical volume of the droplet detachment. With an increase in the applied voltage the electric force dominates the surface force, i.e., the surface tension, which is acting against the electric force [27]. A gradual change in the shape of the drop was observed, and also the dripping rate was increased with an increase in the applied voltage. Uniform size droplets appeared with a regular formation interval up to 2.80 kV, and then a rapid decrease in the droplet size was observed at 2.85 kV. Finally a thin jet emanated when the voltage reached to 3.0 kV. At this point the electric forces, produced as a result of the applied voltage, were enough to overcome the surface tension of the liquid to form a jet. The jet showed more stability when the applied voltage was increased to 3.5 kV. The same behavior was observed for solutions A, C, and D, the results for the solution B are provided only because of better droplet capture by the camera.

Fig. 3 illustrates the stable jets of solution D, produced with increasing voltage of 1.3 kV – 1.65 kV and pressure of 27.7 kPa, while Fig. 4 provides that for ethanol with increasing voltage of 1.8 kV – 2.2 kV and under an applied pressure of 0.4 kPa. The results show a similar behavior of the liquids in response to an increase in the applied voltage. Below these ranges of voltage the solutions were unable to form stable jets, because the electric

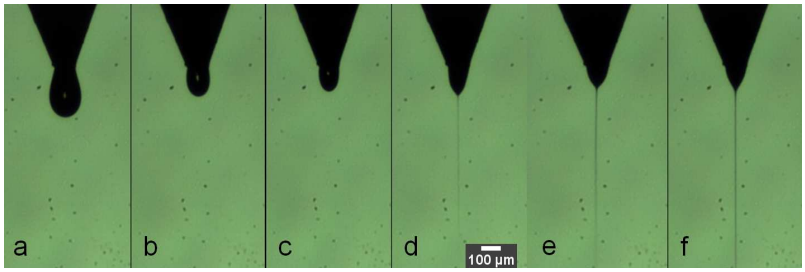

FIG. 2: Deformation behavior of solution B at pressure 0.7 kPa with increasing applied voltage: (a) 2.74 kV, (b) 2.80 kV, (c) 2.85 kV, (d) 3.0 kV, (e) 3.3 kV, (f) 3.5 kV.

forces were unable to overcome the surface tension. Once a stable jet is formed, then with a gradual increase in the applied voltage, the conical base of the stable jet gradually contracts and the cone angle gets wider with a decrease in the height of the cone. This behavior is the result of the system trying to minimize its energy [27]. With an increase in the applied pressure of 0.1 kPa – 0.2 kPa at a voltage of 2.0 kV an increase in the jet diameter was observed for ethanol (Fig. 5).

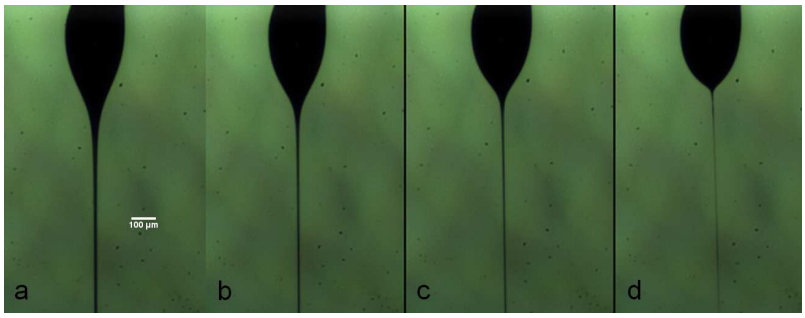

FIG. 3: Stable jets of solution D at increasing applied voltage under the applied pressure of 27.7 kPa: (a) 1.3 kV, (b) 1.45 kV, (c) 1.60 kV, (d) 1.65 kV.

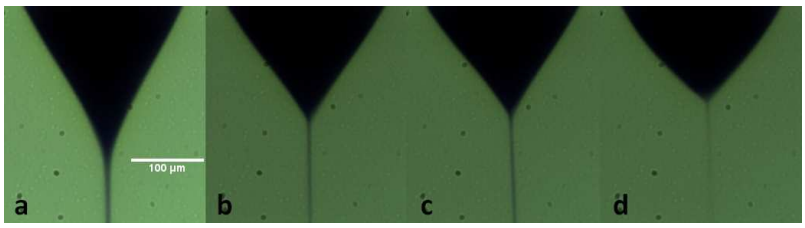

FIG. 4: Stable jets of ethanol at increasing applied voltage and under the applied pressure of 0.4 kPa: (a) 1.8 kV, (b) 1.9 kV, (c) 2.0 kV, (d) 2.2 kV.

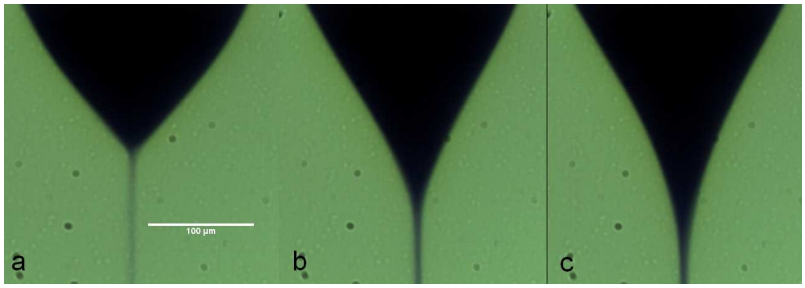

FIG. 5: Deformation behavior of ethanol at 2.0 kV with increasing applied pressure: (a) 0.1 kPa, (b) 0.2 kPa, (c) 0.4 kPa.

III-1-2. Effect of the bias and pulse voltage

Fig. 6 shows the deformation of the meniscus when only the bias voltage was applied. The height of the meniscus was gradually increased with a gradual increase of the bias voltage from 1.1 kV to 1.5 kV. The meniscus reached to its maximum height at 1.5 kV, but no jet formation was observed. When the pulse voltage was applied to the meniscus, further deformations were induced, and these deformations were very much related to the applied bias voltage and pulse time (Table II). Fig. 7 shows the effect of meniscus deformation when the pulse voltage of 0.9 kV was applied with a bias voltage of 1.4 kV. Before the pulse voltage was applied, the meniscus was unable to show any jetting behavior, but with the application of the pulse voltage the dripping mode was observed. The meniscus was further transformed from the dripping mode to the pulsating jet mode with an increase in the pulse time of 2 ms – 50 ms. When the applied bias voltage was raised to 1.5 kV the meniscus showed a higher deformation with an increase in the duty cycle (Fig. 8). The results of this experiment reveal that a cone jet can be produced directly with the application of pulse voltages of large values superimposed on a bias voltage, and also confirms that higher bias voltages along with a pulse voltage of higher values of pulse time are required to create a stable cone jet.

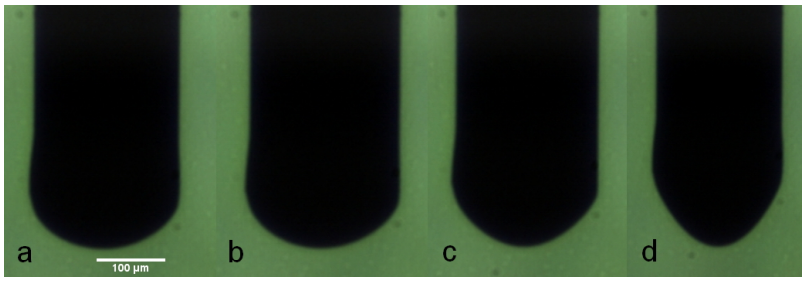

FIG. 6: Effect on the meniscus with increasing applied voltage: (a) 1.10 kV, (b) 1.25 kV, (c) 1.40 kV, (d) 1.50 kV; applied pressure = 0.2 kPa.

Table III represents the effect of a pulse voltage on the meniscus deformation with the applied bias voltage of 1.5 kV. Figure 9 shows the meniscus deformation due to the

TABLE II: Effect of bias voltage on the deformation of the meniscus with a pulse voltage of 0.9 kV, under the applied pressure of 0.2 kPa and frequency of 100 Hz.

Pulse voltage	Bias voltage	Pulse time (ms)	Figure No.	Jet mode
0.9 kV	1.4 kV	2	7 (c)	Dripping mode
		4	7 (d)	Pulsating jet
		5	7 (e)	Pulsating jet
0.9 kV	1.5 kV	4	8 (c)	Stable jet
		5	8 (d)	Stable jet

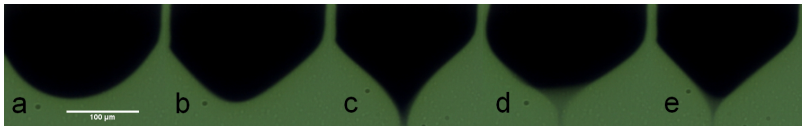

FIG. 7: Meniscus deformation under the applied pressure of 0.2 kPa with bias voltage alone (a) 1.35 kV, (b) 1.4 kV, and under a bias voltage of 1.4 kV with pulse voltage of 0.9 kV having pulse time: (c) 2 ms, (d) 4 ms, (e) 5 ms.

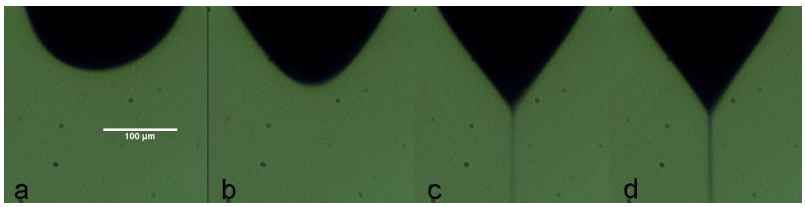

FIG. 8: Meniscus deformation with bias voltage alone of (a) 1.45 kV, (b) 1.5 kV, and under a bias voltage of 1.5 kV with a pulse voltage of 0.9 kV having pulse time: (c) 4 ms, (d) 5 ms, and applied pressure = 0.2 kPa.

effect of a 0.75 kV pulse voltage superimposed on a bias voltage of 1.5 kV. The operating mode transformed from a dripping mode to a finer pulsating jet with an increase in the pulse time of 2 ms – 5 ms. The pulse voltage was then increased to 0.8 kV with increasing pulse time of 4 ms and 5 ms. As shown in Fig. 10, the meniscus showed a pulsating jet behavior under these parameters. Finally the pulse voltage was increased to 0.9 kV with a pulse time of 4 ms and 5 ms. This increase in pulse voltage with higher values of the pulse time transformed the operating mode from pulsating jet to stable cone jet mode (Fig. 8). The experiments showed that bias voltage alone was not sufficient to generate any jetting behavior until the pulse voltage with an optimum value of pulse time was applied.

TABLE III: Effect of the pulse voltage on the deformation of the meniscus with a bias voltage of 1.5 kV, under the applied pressure of 0.2 kPa and frequency of 100 Hz.

Bias voltage	Pulse voltage	Pulse time (ms)	Figure No.	Jet mode
1.5 kV	0.75 kV	2	9 (b)	Dripping mode
		4	9 (c)	Dripping mode
		5	9 (d)	Pulsating jet
1.5 kV	0.80 kV	4	10 (b)	Pulsating jet
		5	10 (c)	Pulsating jet
1.5 kV	0.90 kV	4	8 (c)	Stable jet
		5	8 (d)	Stable jet

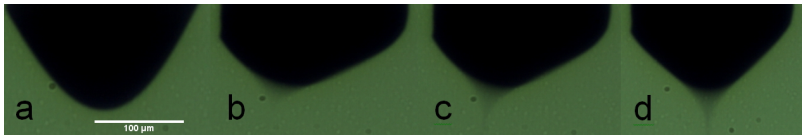

FIG. 9: Meniscus deformation with a bias voltage alone (a) 1.5 kV, and deformation under a bias voltage of 1.5 kV with a pulse voltage of 0.75 kV having pulse time: (b) 2 ms, (c) 4 ms, (d) 5 ms; the applied pressure = 0.2 kPa.

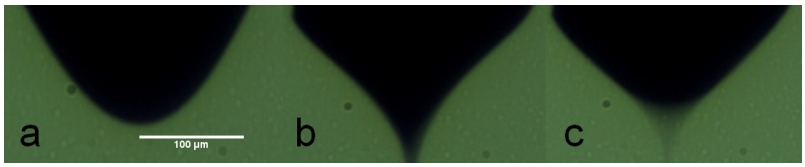

FIG. 10: Meniscus deformation with a bias voltage alone (a) 1.5 kV, and deformation under a bias voltage of 1.5 kV with a pulse voltage of 0.80 kV having pulse time: (b) 4 ms, (c) 5 ms; the applied pressure = 0.2 kPa.

III-2. Effect of the Liquid Conductivity and Viscosity

The liquid conductivity and viscosity has a marked effect on both the jet stability and the shape of the liquid cone by controlling the amount of electric charge on the surface of the liquid [21]. All the liquids mentioned in Table I showed deformation into a stable cone jet under specific values of electric field, pulse time, applied pressure, and frequency. In order to evaluate the effect of these parameters on jet stability, solutions A, B, and D were selected for experimentation. The behavior of the jet stability was examined under different values of the applied pressure. Fig. 11 shows the relationship between the critical voltages required for stable jet formation and the applied pressure for three different conductivity liquids A, B, and D. The general trend which appeared as a result of the experiment showed

that with an increase in applied pressure the critical voltage decreased.

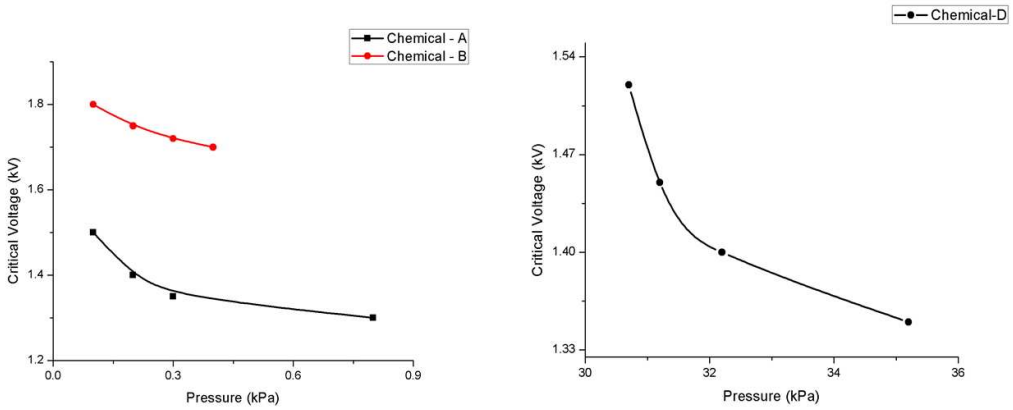

FIG. 11: Critical voltage dependency on the applied pressure for liquids of different conductivities.

Solution A having high conductivity and low viscosity and low surface tension was tested with a pulse voltage of 1 kV superimposed on the bias voltage of 1.3 kV (Table IV). The cone jet transition occurs only when the surface tension is overcome by the electrical force near the conical apex, and thus the critical potential required for the cone jet transition is higher for the liquids with high surface tension [21]. At the optimum voltage, i.e., a bias voltage of 1.3 kV and pulse voltage of 1 kV, the surface tension of the liquid which opposed the formation of a stable cone jet is overcome by electrical forces. The solution was able to form a stable cone jet both at low and high frequencies. At a frequency of 100 Hz the solution was able to deform into a stable cone jet for all the values of the pulse time (2 ms – 8 ms) and also showed stable jet behavior for all the values of pulse time (0.8 ms – 3.2 ms) at a frequency of 250 Hz. At a frequency of 600 Hz the transition mode transformed from an intermittent jet to a stable jet with an increase in the pulse time of 0.32 ms – 1.28 ms, and similarly at 700 Hz the solution transformed from an intermittent jet to a pulsating jet and then to a stable jet mode with an increase in the duty pulse time of 0.142 ms – 0.710 ms. Solution D having low conductivity and high viscosity and high surface tension as compared to solution A was tested with the pulse voltage of 1 kV superimposed on the bias voltage of 1.5 kV, and this was enough to overcome the opposing surface tension to form a stable cone jet. At higher frequencies the solution was unable to transform into a stable cone jet transition mode easily. At a frequency of 50 Hz and 100 Hz the solution showed stable jet behavior with an increase in the pulse time of 4 ms – 16 ms and 2 ms – 8 ms, respectively. The transition mode transformed from intermittent jetting to a pulsating jet and then to a stable jet mode with an increase in the duty pulse time of 0.16 ms – 0.8 ms at a frequency of 600 Hz, and similar behavior was observed at a frequency of 700 Hz (Table IV). Solution C showed almost a similar behavior as solution D in response to these

operating parameters. The reason for this behavior can be explained by

$$\tau_c = \frac{\varepsilon_0 \varepsilon_r}{K}, \tag{1}$$

$$\tau_H = \frac{\eta r_c}{\gamma}, \tag{2}$$

$$f_{\text{Rayleigh}} = \frac{1}{2\pi}\left[\frac{8\gamma}{\rho r^3}\right]^{\frac{1}{2}}, \tag{3}$$

$$t_{\text{Rayleigh}} = \frac{1}{f_{\text{Rayleigh}}}, \tag{4}$$

where τ_c and τ_H represents the charge relaxation time and hydrodynamic relaxation time, ε_r is the dielectric constant, and K represents the conductivity; η is the viscosity and γ is the surface tension of the liquid. Here r_c is the radius of the outer diameter of the capillary, which is 210 μm in our case, f_{Rayleigh} is the natural frequency of the pendant drop, and t_{Rayleigh} is the Rayleigh time, which is the minimum time required for a stable jet mode and uniform drop formation; ρ is the density of the solution and r is the radius of the pendant droplet.

The charge relaxation time represents the duration required for a meniscus to acquire an equilibrium state during the electrohydrodynamic jetting phenomena. The Rayleigh formula is used to measure the natural frequency of the pending droplet, and the hydrodynamic relaxation time represents the damping effects. Liquids with very low conductivities have insufficient charges in the bulk to create enough surface charge, resulting in a long relaxation time, and due to this the liquid is unable to develop an appreciable electrical stress to counteract the surface tension. As a result the pendant droplet simply grows in volume and finally drips off instead of forming a stable cone jet. On the other hand, when the conductivity is too high, then the charge relaxation time is too small. In this case the surface charge exceeds the Rayleigh limit before the formation of the droplet. A normal stress is applied on the surface of the droplet due to the surface charge, which alone is not enough to produce a stable cone jet. Also the high surface charge carried by the highly conductive liquids introduces a large radial electric field which results in destabilization of the jet [21].

For a liquid to form a stable cone jet, its charge relaxation time should be smaller than the hydrodynamic relaxation time. All the solutions used in this experiment obey this law by having a charge relaxation time smaller than the hydrodynamic relaxation time (Table I), and thus all of them formed stable cone jets under specific values of applied voltage, pressure, pulse time, and frequency. Also the pulse time for any solution should be greater than both the hydrodynamic relaxation time as well as the Rayleigh time in order to form stable cone jets. If the pulse time is less than any one of these parameters then stable cone jets will not form. The rate at which the charge accumulates on the surface

TABLE IV: Effect of frequency and duty cycle on the deformation of the meniscus. A pulse voltage of 1 kV superimposed on the bias voltage of 1.3 kV was used under the pressure of 0.8 kPa for solution A, and for solution D a pulse voltage of 1 kV superimposed on a bias voltage of 1.5 kV was used at 32.2 kPa pressure.

Sample Name	t_{Rayleigh} (ms)	Frequency (Hz)	Pulse time (ms)	Jet mode
Solution A	0.45	100	2	Stable
			5	Stable
			8	Stable
		250	0.8	Stable
			1.6	Stable
			3.2	Stable
		600	0.32	Intermittent
			0.80	Stable
			1.28	Stable
		700	0.142	Intermittent
			0.284	Intermittent
			0.426	Pulsating
			0.710	Stable
Solution D	0.37	50	4	Stable
			10	Stable
			16	Stable
		100	2	Stable
			5	Stable
			8	Stable
		600	0.16	Intermittent
			0.32	Pulsating
			0.48	Pulsating
			0.80	Stable
		700	0.142	Intermittent
			0.284	Intermittent
			0.426	Pulsating
			0.710	Stable

of the meniscus depends upon the relaxation time of the liquid [21]. With an increase in the applied pressure the amount and flow of charges towards the meniscus is increased, due to which the charge accumulation over the surface of the meniscus is increased and the relaxation time is decreased, resulting in a low critical voltage required for the formation of a stable jet (Fig. 11).

Solution A was able to deform into a stable cone jet for all the values of the pulse time at a frequency of 100 Hz and 250 Hz because of the sufficient charge relaxation time, due to its high conductivity and sufficient hydrodynamic relaxation time, which is due to its low viscosity and also the pulse time being greater than both the Rayleigh time as well as the hydrodynamic relaxation time to overcome the damping effects (Table IV). At 600 Hz intermittent jet behavior was observed for a pulse time of 0.32 ms, which is less than t_{Rayleigh} and τ_H of the solution. The fluid underwent a change in transition mode when the pulse time was raised to 0.8 ms. Now the duty cycle is well above the values of t_{Rayleigh} and τ_H and thus the solution started to show a stable jet transition mode. At 700 Hz an intermittent jet behavior was observed for the low pulse time of 0.142 ms – 0.284 ms, but when the pulse time reaches closer to t_{Rayleigh} the transition mode transforms from intermittent to a pulsating jet mode, and at 0.71 ms of pulse time a stable jet mode is observed, because of sufficient charge relaxation time and hydrodynamic relaxation time. Solution D with the highest viscosity was unable to form stable cone jets easily at higher frequencies because of its high charge relaxation time and hydrodynamic relaxation time. At 50 Hz and 100 Hz a stable cone jet transition mode was achieved at pulse time of 4 ms – 16 ms and 2 ms – 8 ms, respectively. This is because the pulse time is much higher than t_{Rayleigh} and τ_H, and because of the sufficient relaxation time at this stage. At 600 Hz, when the pulse time approaches closer to t_{Rayleigh} and τ_H, then the transition mode transforms from intermittent to a pulsating jet, and it forms a stable jet when the pulse time is long enough, i.e., 0.8 ms. Similarly, at 700 Hz the solution showed an intermittent behavior at and below 0.142 ms pulse time, and a pulsating jet behavior was observed at a pulse time of 0.284 ms, but it showed a stable jet mode at and above 0.71 ms pulse time, because this value is higher than both t_{Rayleigh} and τ_H (Fig. 12).

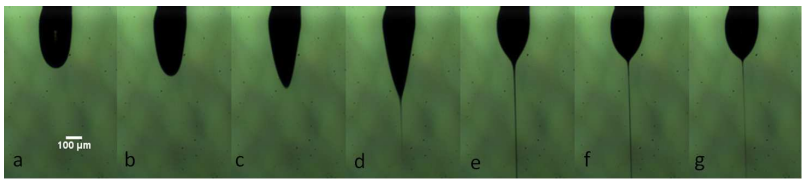

FIG. 12: Meniscus deformation of solution D with a pulse voltage of 1 kV superimposed on a bias voltage of 1.5 kV under the applied pressure of 32.2 kPa and frequency of 700 Hz having pulse time: (a) 0.071 ms, (b) 0.142 ms, (c) 0.284 ms, (d) 0.426 ms, (e) 0.710 ms, (f) 0.994 ms, (g) 1.136 ms.

The results of this experiment confirm that the conductivity and viscosity have a major role in stabilization of the jet. The ionic mobility in a highly viscous medium is low, which results in a decrease of both the conductivity and radial electric field and contributes to the jet stabilization [21]. The critical voltage required for the formation of a stable cone

jet depends mainly upon the surface tension of the liquid. Liquids with high surface tension require higher values of the critical potential to achieve a stable cone jet transition mode. The frequency and pulse time of the pulse voltage has a key role in stable jet formation. Unlike low viscous liquids, high viscosity and low conductivity liquids form a stable cone jet at low frequencies with higher values of the pulse time, and at higher frequencies the high viscous liquids are unable to deform into stable cone jets easily. Both kinds of liquids form a stable cone jet only under some optimum values of frequency and pulse time, which are enough to achieve the required charge relaxation time and hydrodynamic relaxation time and the Rayleigh time. The experiment also concluded that under higher values of applied pressure, a stable cone jet transition mode can be achieved at relatively low values of the applied voltage, and this critical voltage decreases with an increase in the applied pressure.

III-3. Designing of Dimensionless Parameters

The formulation of dimensionless physical parameters to guide the analysis of the result greatly helps in better understanding of the EHD phenomenon. We have made attempts by conducting experiments to design the dimensionless groups that affect the EHD jetting. The formulated dimensionless parameters have been thoroughly analyzed to check their effects on the EHD jetting.

The identified main variables of the EHD process are: the applied voltage (V_a), applied pressure (P_a), distance between the nozzle and counter electrode (l), diameter of the nozzle (d), viscosity of the solution (η), conductivity of the solution (K), dielectric constant of the solution (k), surface tension of the solution (γ), and density of the solution (ρ). Therefore, we have nine variables and four dimensions: mass (M), time (T), length (L), and charge (C).

According to the Buckingham Π theorem [28], the total number of dimensionless groups (A) is equal to the number of variables (B) minus the number of dimensions (C), i.e.,

$$\mathrm{A} = \mathrm{B} - \mathrm{C} = 9 - 4 = 5.$$

The following five dimensionless parameters were designed:

$$\mathrm{A}_1 \sim \mathrm{A}_5 = \left\{ \frac{\tau_c}{\tau_H}, k, \frac{d}{l}, \alpha, \beta \right\}.$$

A_1 is the ratio between two characteristic times, i.e., the charge relaxation time Eq. (1) and the hydrodynamic relaxation time Eq. (2). These times are important for determining the jetting system. The EHD phenomena must satisfy the condition of $\frac{\tau_c}{\tau_H} < 1$ in order to get a stable cone jet [29]. A_2 is the dielectric constant of the solution and represents the material properties. As every solution has only one value of the dielectric constant, and it was kept constant in the experimentation; therefore, its effect on EHD jetting was not investigated. A_3 is the geometrical representation and is the ratio between the nozzle diameter and nozzle counter electrode distance. A_4 and A_5 represent the processing conditions. $\mathrm{A}_4 = \frac{P_a}{P_c} = \alpha$ is the dimensionless applied pressure and is the ratio of the applied pressure to the critical

pressure. The critical pressure is the pressure at which the solution forms a stable cone jet. A_5 is the dimensionless voltage and is the ratio between the applied voltage V_a and the critical voltage V_c. The critical voltage is the voltage at which the stable cone jet is achieved.

The magnitude of A_1, which is the ratio of the charge relaxation time to hydrodynamic relaxation time, determines the jetting system. The liquid must satisfy the condition of $\frac{\tau_c}{\tau_H} < 1$ in order to form a stable cone jet. As an example from the experimental analysis, the dimensionless parameter $(\frac{\tau_c}{\tau_H})$ of the solution D and ethanol is 0.18 and 0.92 respectively, which is less than 1 and therefore resulted in the formation of stable cone jets (Fig. 3 and Fig. 4). All the solutions used in the study satisfied these conditions and therefore formed stable cone jets.

The dimensionless parameter A_3 showed a great effect on the EHD jetting system. The results showed that an optimum value of A_3 is required to achieve a stable cone jet. Fig. 13 shows the effect of A_3 on the jetting behavior for solution B. The solution showed a stable cone jet mode at $A_3 = 0.055$, i.e., when the distance between the nozzle and substrate was kept at 2000 μm (2 mm). The solution showed a pulsating jet mode at the A_3 value of 0.073 and showed no jetting at all when the A_3 value was reduced to 0.044. This shows that the dimensionless parameter of $A_3 = 0.055$ is the optimum value for the solution B to form a stable cone jet under the applied voltage and pressure of 3.5 kV and 0.7 kPa, respectively.

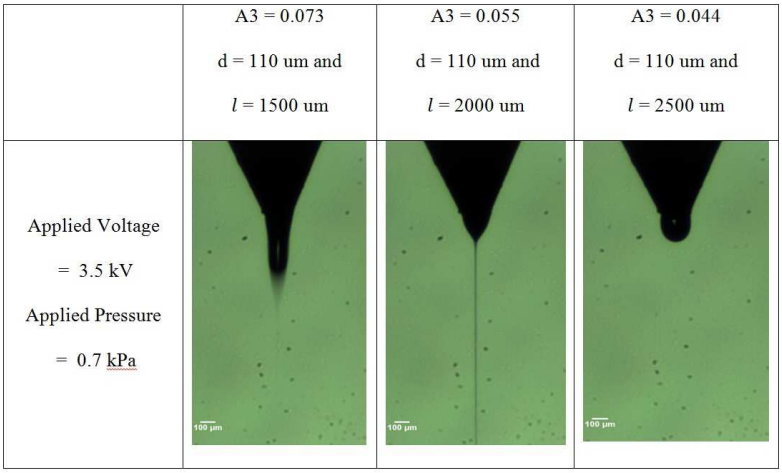

FIG. 13: The effect of A_3 on the jetting behavior for solution B.

The dimensionless applied pressure and voltage were also investigated to check their influence on the EHD jetting. The critical voltage and critical pressure have been calculated experimentally. The critical voltage and critical applied pressure for solution B was 3.5 kV and 0.7 kPa, respectively. Similarly the V_c and P_c for the ethanol were 2.0 kV and 0.4 kPa, respectively. The results showed that the dimensionless voltage and applied pressure greatly affects the jetting system (Fig. 14). Both the ethanol and solution B showed a stable cone

jet mode at an optimum value of $\beta = 1$ at $\alpha = 1$. The operating mode transformed from a stable cone jet to multi-jet when the value of the dimensionless β was raised to 1.5 and showed a pulsatimg jet mode at $\beta = 0.5$. Therefore, the results lead to the conclusion that the dimensionless voltage (β) as well as the pressure (α) affects the EHD jetting behavior significantly.

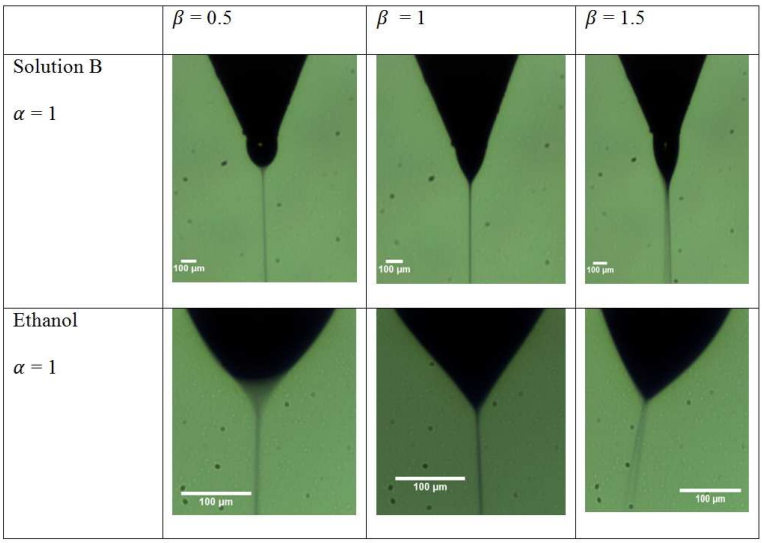

FIG. 14: The effect of the dimensionless voltage and applied pressure on the jetting behavior of ethanol and solution B.

IV. CONCLUSIONS

The results of the experiments lead to the conclusion that each property of the liquid, such as the conductivity, surface tension, and viscosity, has a unique and prominent role in electrohydrodynamic jetting. The critical voltage required for the formation of the stable cone jet greatly depends upon the surface tension of the liquid. High surface tension liquids require a high critical potential to overcome the surface tension of the liquid in order to form a stable jet. The conductivity and viscosity both effect the stabilization of the jet. The radial electric field, which destabilizes the jet, decreases due to low ionic mobility in highly viscous liquids, and thus viscosity helps in jet stabilization. Both the bias voltage and pulse voltage along with pulse time are important for the electrohydrodynamic jetting. Under the effect of bias voltage the meniscus reached to its maximum height without the formation of a jet. A pulse voltage with an optimum value superimposed on a bias voltage results in jetting. The pulse voltage gives rise to tangential electric stress on the meniscus, which helps in jet formation. Pulse voltage with a small pulse time creates a dripping mode, and, with an increase in duty cycle, the transition mode transform from dripping to a stable

cone jet mode. Unlike low viscous liquids, high viscous liquids having low conductivity are unable to form stable jets easily at higher frequency and low pulse time. This is because of the insufficient charge relaxation time and hydrodynamic relaxation time required for the formation of a stable cone jet. The designed dimensionless parameters of $(\frac{\tau_c}{\tau_H}, \frac{d}{l}, \alpha, \beta)$ showed great effect on the EHD jetting and can be used to guide the analysis of the results.

Acknowledgment

This study was supported by a grant from Technology Innovation Program (No. 10041596, Development of core technology for TFT free active matrix addressing color electronic paper with day and night usage) funded by the Ministry of Knowledge Economy (MKE, Korea).

References

[1] T. R. Hebner, C. C. Wu, D. Marcy, M. H. Lu, and J. C. Sturm, Appl. Phys. Lett. **72**, 519 (1998). doi: 10.1063/1.120807
[2] T. Goldmann and J. S. Gonzalez, J. Biochem. Biophys. Methods **42**, 105 (2000). doi: 10.1016/S0165-022X(99)00049-4
[3] D. B. Chrisey, Science **289**, 879 (2000). doi: 10.1126/science.289.5481.879
[4] J. U Park *et al.*, Nat. Mater. **6**, 782 (2007). doi: 10.1126/science.289.5481.879
[5] S. N. Jayasinghe and M. J. Edirisinghe, J. Aerosol. Sci. **33**, 1379 (2002). doi: 10.1016/S0021-8502(02)00088-5
[6] D. A. Saville, Phys. Fluids **14**, 1095 (1971). doi: 10.1063/1.1693569
[7] K. H. Choi, K. Rahman, A. Khan, and D. S. Kim, J. Mech. Sci. Technol. **25**, 1 (2011). doi: 10.1007/s12206-011-0333-z
[8] D. S. Kim, K. Rahman, A. Khan, and K. H. Choi, to appear in Mater. Manuf. Process. doi: 10.1080/10426914.2012.663121
[9] K. H. Choi *et al.*, *Recent Advances in Nanofabrication Techniques and Applications*, ed. B. Cui (InTech. Rijeka, Croatia, 2011) Chap. 27.
[10] K. Rahman, J. B. Ko, S. Khan, D. S. Kim, and K. H. Choi, J. Mech. Sci. Technol. **24**, 307 (2010). doi: 10.1007/s12206-009-1149-y
[11] K. Rahman, A. Khan, N. M. Nam, K. H. Choi, and D. S. Kim, Int. J. Precis. Eng. Manuf. **12**, 663 (2011). doi: 10.1007/s12541-011-0086-8
[12] N. M. Muhammad *et al.*, Curr. Appl. Phys. **11**, S68 (2011).
[13] N. M. Muhammad, N. Duraisamy, D. S. Kim, and K. H. Choi, Thin Solid Films **520**, 1751 (2012). doi: 10.1016/j.tsf.2011.08.065
[14] K. H. Choi, M. Mustafa, K. Rahman, J. B. Ko, and Y. H. Doh, Appl. Phys. A-Mater. Sci. Process. **106**, 165 (2012).
[15] A. Khan, K. Rahman, D. S. Kim, and K. H. Choi, J. Mater. Process. Technol. **212**, 700 (2012). doi: 10.1016/j.jmatprotec.2011.10.024
[16] D. S. Kim *et al.*, Mater. Manuf. Process. **26**, 1196 (2011). doi: 10.1080/10426914.2011.551956
[17] A. Khan, K. Rahman, M. T. Hyun, D. S. Kim, and K. H. Choi, Appl. Phys. A-Mater. Sci. Process. **104**, 1113 (2011).

[18] K. H. Choi *et al.*, J. Micromech. Microeng. **20**, 075033 (2010). doi: 10.1088/0960-1317/20/7/075033
[19] S. Khan *et al.*, Curr. Appl. Phys. **11**, S271 (2011). doi: 10.1016/j.cap.2010.11.044
[20] J. Choi *et al.*, Appl. Phys. Lett. **93**, 193508 (2008). doi: 10.1063/1.3020719
[21] H. F. Poon, PhD. Thesis, (Princeton University, Princeton, 2002).
[22] M. M. Hohman, M. Shin, G. Rutledge, and M. Brennera, Phys. Fluids **13**, 2201 (2001).
[23] M. W. Lee *et al.*, J. Aerosol. Sci. **46**, 1 (2012).
[24] J. Kim, H. Oh, and S. S. Kim, J. Aerosol. Sci. **39**, 819 (2008). doi: 10.1016/j.jaerosci.2008.05.001
[25] A. Barrero, A. M. Gañán-Calvo, J. Dávila, A. Palacios, and E. Gómez-González, J. Electrost. **47**, 13 (1999). doi: 10.1016/S0304-3886(99)00021-2
[26] M. Cloupeau and B. Prunet-foch, J. Aerosol. Sci. **25**, 1021 (1994). doi: 10.1016/0021-8502(94)90199-6
[27] I. Hayati, A. I. Bailey, and T. F. Tadros, J. Colloid Interface Sci. **117**, 205 (1987). doi: 10.1016/0021-9797(87)90185-8
[28] J. M. Kay and R. M. Nedderman, *Fluid Mechanics and Transfer Processes* (Cambridge University Press, 1990). 384–386.
[29] A. M. Gañán-Calvo, J. Dávila, and A. Barrero, J. Aerosol. Sci. **28**, 249 (1997). doi: 10.1016/S0021-8502(96)00433-8